BULK HYDROGENATION OF MC SILICON MATERIALS AND SOLAR CELLS: FROM RESEARCH LAB TO PV-INDUSTRY

T. Pernau, G. Hahn, M. Spiegel, G. Dietsche

Universität Konstanz, Fachbereich Physik, Fach X916, 78457 Konstanz, Germany
Tel.: +49-7531-88-3644, Fax: +49-7531-88-3895
E-mail: Thomas.Pernau@uni-konstanz.de

ABSTRACT: Today more than 50% of the crystalline PV modules are based on multicrystalline silicon (mc Si), making defect passivation by hydrogenation an important issue in solar cell processing. The diffusion of hydrogen into the bulk due to MIRHP (Microwave Induced Remote Hydrogen Plasma) passivation and the diffusion of hydrogen out of the bulk due to different annealing steps were investigated indirectly by spectral response and illuminated I-V measurements of solar cells made on two ribbon silicon materials (EFG from RWE Solar (former ASE) and RGS originally developed by Bayer AG) and one block casted mc Si material (Baysix from Deutsche Solar). We observed that both processes - diffusion and effusion of hydrogen - are strongly dependent on the material, especially on the interstitial oxygen concentration $[O_i]$. For materials with high $[O_i]$ high optimum passivation temperatures and long passivation times have been found, whereas for materials with low $[O_i]$ care has to be taken to avoid hydrogen effusion during proceeding processing steps, e.g. by using a capping layer during the contact firing step. Based on these investigations we developed an integrated MIRHP/LPCVD (Low Pressure Chemical Vapor Deposition) process for high throughput processing of mc Si solar cells.
Keywords: Ribbon Silicon - 1: Multi-Crystalline - 2: Passivation – 3

1. INTRODUCTION

The increasing importance of multicrystalline silicon for photovoltaics makes defect passivation techniques such as bulk hydrogenation an important issue in mc Si solar cell technology. With ribbon silicon entering the market but having lower starting quality due to a higher concentration of crystal defects, bulk passivation gains even more importance. Various techniques have been investigated for bulk hydrogenation (H-ion-implantation [1], direct H-plasma [2] and damage free hydrogenation [3,4]). We are focusing on a microwave induced remote hydrogen plasma (MIRHP) technique suggested in the mid 80's [3] and used at University of Konstanz [4,5] and other research institutes [ref. in [6]] since the last decade.

The purposes of our work was the study of H-diffusion phenomena in three different multicrystalline silicon materials and the application of the obtained knowledge for the integration of bulk hydrogenation into industrial solar cell processes. An industrial-type LPCVD (low pressure chemical vapour deposition) reactor was modified to perform hydrogen passivation using the MIRHP technique. Several varieties of an integrated LPCVD+MIRHP process (LPCVD+H) were tested.

2. INVESTIGATED MATERIALS

For the investigation two ribbon silicon materials (EFG (Edge-defined Film-fed Growth, [7]) and RGS (Ribbon Growth on Substrate, [8]) as well as one block casted mc silicon material (Baysix) have been chosen. Differences of the used crystallisation techniques result in a large variety of structural defects (interstitial oxygen concentration $[O_i]$, substitutional carbon concentration $[C_s]$ and dislocation density DD) and as grown bulk minority carrier diffusion length L_{diff} as shown in table I.

For all these materials bulk passivation is needed to decrease the costs per W_p to an economically acceptable level. Many cell manufacturers using block-cast mc wafers and RWE Solar using the EFG material are applying a contact firing process through a hydrogen rich PECVD SiN antireflective coating which produces an efficient hydrogenation included in the processing sequence. In the PECVD firing-through process bulk and surface passivation are determined by SiN composition and it is not possible to seperate them.

The RGS material is currently still in the R&D phase but has been taken for the investigation due to its good prospects to reduce costs for future solar cell production [8] and due to its sensitivity to hydrogenation [9,10].

Table I: Properties of the materials used for this study.

Material	$[O_i]$ $[cm^{-3}]$	$[C_s]$ $[cm^{-3}]$	DD $[cm^{-2}]$	L_{diff} $[\mu m]$
Baysix	$3*10^{17}$	$3*10^{17}$	10^4-10^6	~100
EFG	$<10^{17}$	10^{18}	10^4-10^8	20-100
RGS	2-$3*10^{18}$	10^{18}	10^5-10^7	<20

3. MIRHP PASSIVATION

For the experiments small 4 cm² solar cells without antireflective coating (flat untextured surface) have been used. After the emitter formation and a thin dry thermal oxidation for surface passivation the back side is formed by evaporating 2 μm Al and a subsequent alloying step. The front grid was defined by standard photolithography and evaporation of Ti/Pd/Ag. Finally the E-gun damage of the front surface has been healed by forming gas annealing.

The MIRHP passivation technique used in this study for the finished solar cells after cell separation using a dicing saw is well described in literature [4]. By separating the generation of H atoms from the location of H-diffusion into the cell the MIRHP process does not seriously damage the surface of the cell like most of the other H-passivation

techniques such as hydrogen ion implantation [1] and direct hydrogen plasma passivation [2].

In figure 1 the change in J_{sc} for cells made from the three different materials in dependency on the MIRHP passivation time is shown (passivation temperature: 350 °C). For comparison reasons, J_{sc} is normalised to the values of the unpassivated cells, respectively (EFG: 19.0, Baysix: 22.6, RGS: 10.1 mA/cm^2). Obviously, in the defect rich ribbons a higher increase can be obtained due to a higher defect density. But the diffusion velocity seems to be dependant on the interstitial oxygen concentration present in the material (table 1), as saturation is reached in EFG at first with Baysix following and RGS reaching saturation only after up to 10 h passivation time. This is in agreement with former studies carried out on wafers using the same production technique with only the interstitial oxygen concentration as a parameter. E.g. SIMS measurements on multicrystalline wafers taken from different positions within one ingot with different oxygen concentrations showed that with increasing O_i concentration the deuterium diffusion during a direct plasma hydrogenation is slowed down [11]. In another study RGS material with differing O_i concentrations revealed the same behaviour [12].
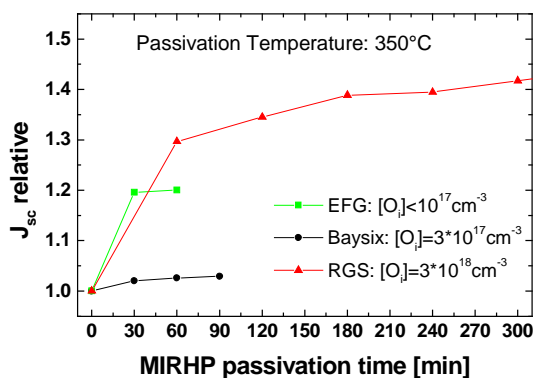

Figure 1: J_{sc} behaviour in dependency on passivation time for the materials under investigation.

4. H-EFFUSION

In another experiment we examined the diffusion out of H-passivated solar cells. The results from this experiment are important when the cell is exposed to elevated temperatures after the H-passivation step within the solar cell process. If the hydrogen diffuses out of the cell during a subsequent temperature step, the passivation effect will be weakened resulting in a decrease in cell efficiency. Therefore we annealed the cells inside the quartz tube normally used for the MIRHP passivation in N_2-ambient (without H-plasma) at different temperatures for 15 min, respectively. The results from this experiment can be seen in figure 2. Here the J_{sc} values are normalised to the values of the passivated cells. J_{sc} for the unpassivated cells (directly after cell processing) as well as the data after MIRHP passivation (before annealing) are listed in table II. The cells used for this study are not the same as the ones used in the previous section.
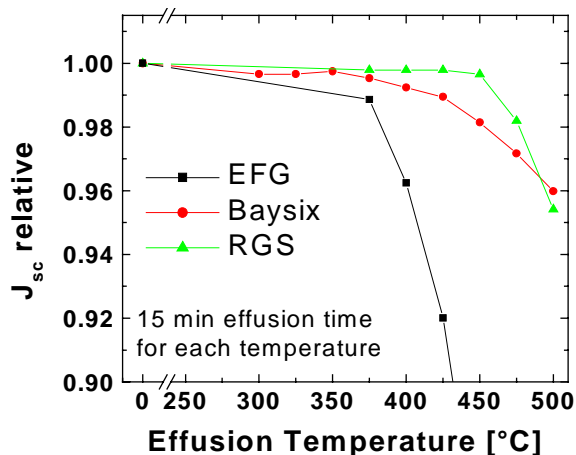

Figure 2: Behaviour of J_{sc} for three H-passivated solar cells during annealing steps (no H-plasma) at different temperatures.

Table II: J_{sc} values of the cells from figure 2 directly after processing (unpassivated) and after MIRHP passivation (before annealing).

Cell	unpassivated	passivated
EFG	17.2	22.0
Baysix	22.2	23.7
RGS	12.1	14.4

Again, there is a clear dependency of the out-diffusion temperature on the interstitial oxygen concentration visible. In EFG J_{sc} is already decreased at annealing temperatures <375 °C. A more detailed study for EFG using lower annealing temperatures and longer annealing times revealed that J_{sc} is reduced at temperatures as low as 325 °C [6]. For the Baysix cell with an intermediate O_i concentration the decrease of J_{sc} starts at temperatures around 400 °C, whereas for the RGS cell with a high O_i concentration J_{sc} seems to be stable for temperatures up to 450 °C.

For demonstrating that the decrease of J_{sc} is caused by a reduction of the bulk diffusion length and not by a damage of the front side or the space charge region during the annealing steps, we measured the external quantum efficiencies (EQEs) after the annealing steps. The results at selected temperatures are given in figure 3.

Obviously, for all materials no reduction of the EQE in the short wavelength region (<500 nm) can be detected, while the EQE in the long wavelength part of the spectrum is reduced after the annealing steps in dependency on the annealing temperature. This drop of the EQE is already very pronounced for EFG at a temperature of 400 °C. After an annealing step at 450 °C it can be detected in the Baysix cell as well, whereas it does not appear in the RGS cell at that temperature. Here it can be detected after the annealing at 500 °C, which is in agreement with the results shown in figure 2.
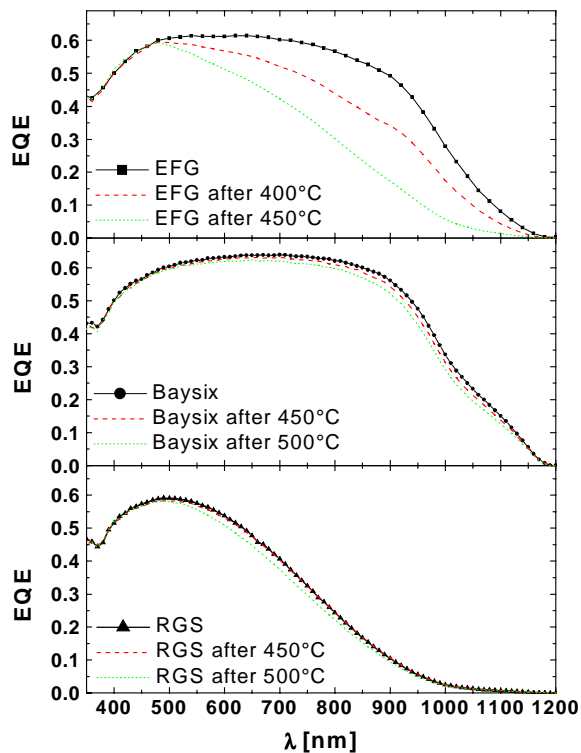
Figure 3: External quantum efficiencies of the passivated cells (symbols) and after two annealing steps. Changes are visible only in the long wavelength region caused by out-diffusion of hydrogen.

The consequences from these experiments are:

- H-diffusion is dependent on the interstitial oxygen concentration of the used wafer with a higher O_i concentration requiring higher passivation temperatures and/or longer passivation times.
- H-passivation has to be optimised for each material according to the O_i concentration.
- Care has to be taken to prevent hydrogen from diffusing out of the cell during subsequent temperature steps. This can be avoided by using a capping layer (e.g. a SiN antireflection coating in combination with a full rear side metallisation) as a diffusion barrier.

5. LPCVD + MIRHP

Each standard LPCVD reactor may easily be upgraded to perform MIRHP processes by adding a gas inlet and a microwave source [13]. The LPCVD+H process should be optimised to a minimum loss of passivation due to effusion, however for a standard LPCVD SiN deposition from dichlorosilane and ammonia temperatures above 700 °C are needed. To keep the thermal load as low as possible, the LPCVD reactor standby temperature was lowered to 400 °C. When heating or cooling, the temperature ramps were performed as fast as possible (heating: 15 °C/min., cooling: 7 °C/min.). In the LPCVD+H processes, hydrogen passivation was performed at standby temperature half an hour before heating up and after cooling down the reactor. Temperature ramps were accompanied by hydrogen plasma to reduce H-effusion.

The flow charts of three selected LPCVD processes are shown in figure 4. All processes use the same recipe for SiN deposition.

For the fabrication of solar cells, SiN was deposited only on one side of the wafers by putting two wafers back-to-back in one boat position. In this case the penetration of hydrogen after SiN deposition is reduced. This problem can be overcome by separating the wafers after SiN deposition (see process LPCVD+H2). The process time of the LPCVD+H processes is approx. 3 h, including the time (1 h) used for hydrogen passivation before heating up and after cooling down plus the time for wafer separation during process LPCVD+H2.
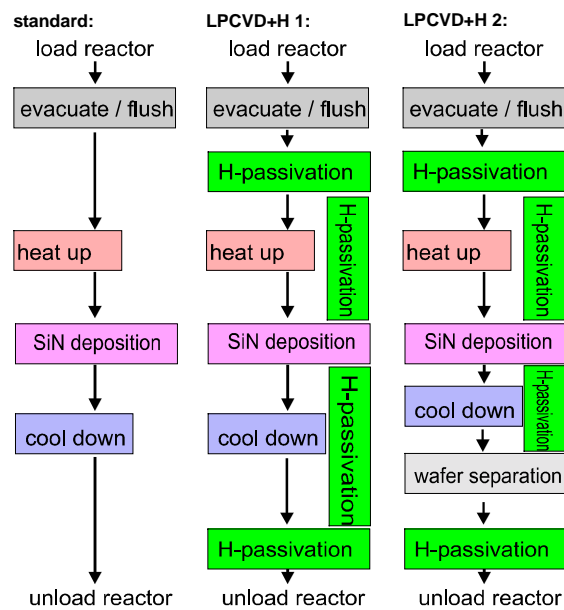

Figure 4: Process flow charts of the standard LPCVD process and two LPCVD+H processes. During the LPCVD+H2 process, the wafers are separated after cooling down for better hydrogen penetration.

The performance of the LPCVD+H processes was investigated by double-sided SiN deposition on bare p-type 10*10 cm² mc Baysix wafers and by single-sided SiN deposition on neighbouring wafers with industrial-type 45 Ω/sq. emitter. The latter were submitted to screen printing (front side Ag paste, rear side Al paste) and firing-through of contacts in a belt furnace. The bare p-type wafers were characterised by μ-PCD measurements after SiN deposition and after firing in the same belt furnace under the same conditions as the solar cells.

Table III: Measured τ_{eff} of neighbouring p-type mc Baysix wafers covered with LPCVD silicon nitride.

SiN Type	τ_{eff} after SiN	τ_{eff} after firing
Standard	2.18 μs	2.23 μs
LPCVD+H 1	3.98 μs	3.49 μs

The effective lifetime of the wafers covered with LPCVD+H silicon nitride is nearly doubled with respect to standard LPCVD silicon nitride, but the measured τ_{eff}-

values are determined by a combination of measured bulk lifetime and surface passivation.

Table IV: Current and voltage analysis of $10*10$ cm^2 industrial type solar cells covered with LPCVD SiN. (statistic: 6 cells per SiN type).

SiN Type	current [mA/cm²]	voltage [mV]
LPCVD+H 1	30.9	599.4
LPCVD+H 2	30.9	599
standard LPCVD	30.8	598.8

The performance gain of the solar cells covered with LPCVD+H silicon nitride is not as high as expected from the lifetime measurements on the bare p-type wafers (table III). A possible reason for this may be the fact that MIRHP included in these LPCVD processes improves mainly surface passivation. The industrial-type 45 Ω/sq. emitter is not very sensitive to an improvement in surface passivation, this might explain the small differences in cell results. A further problem is the fact that the temperature within the inner furnace area after cooling down is higher than 400 °C. This might cause a substantial part of the hydrogen to diffuse out of the cell as investigated in the previous section.

CONCLUSIONS

The microwave induced remote hydrogen plasma (MIRHP) technique was successfully applied for bulk hydrogen passivation of defects in two ribbon silicon materials (RGS and EFG) and one block casted material (Baysix).

We observed that diffusion and effusion of hydrogen are strongly dependent on the material, especially on the interstitial oxygen concentration [O_i]. For RGS with high [O_i] high optimum passivation temperatures and long passivation times have been found, whereas for EFG with low [O_i] care has to be taken to avoid hydrogen effusion during proceeding processing steps, e.g. by using a capping layer during the contact firing step. For Baysix with intermediate [O_i] also an intermediate hydrogen effusion temperature has been observed.

Based on these investigations we started to integrate the MIRHP passivation into a standard LPCVD process for high throughput processing of mc Si solar cells. As a first result, hydrogen passivation nearly doubled τ_{eff} of bare p-type mc Baysix material, whereas processed solar cells were only slightly improved. Regarding the effusion experiments, the temperature of the LPCVD furnace should not exceed 450 °C to avoid hydrogen effusion. We are planning to use alternative reactants for SiN deposition, which allow a reduction of the deposition temperature down to 500 °C. In this case a standby temperature of 350 °C is sufficient, which should lead to better passivation results.

REFERENCES

[1] J.A. Gregory, Z.Y. Vayman, J.I. Hanoka, J. Electrochem. Soc. **136** (1989) 1201.

[2] H.E. Elgamel, S. Sivoththaman, M.Y. Ghannam, J. Nijs, R. Mertens, M. Rodot, D. Sarti, L.Q. Nam, Solar Energy Materials and Solar Cells **36** (1994) 99.

[3] W.L. Hansen, S.J. Pearton, E.E. Haller, Appl. Phys. Lett. **44** (1984) 606.

[4] M. Spiegel, P. Fath, K. Peter, B. Buck, G. Willeke, E. Bucher., Proc. 13th EC PVSEC, Nice (1995) 421.

[5] M. Spiegel, G. Hahn, W. Jooss, S. Keller, P. Fath, G. Willeke, E. Bucher , Proc. 2nd WCPEC, Vienna (1998) 1685.

[6] M. Spiegel, PhD thesis, University of Konstanz (1998).

[7] F.V. Wald, in: Crystals: Growth, Properties and Applications 5 (Springer, Germany, 1981).

[8] H. Lange, I.A. Schwirtlich, Journal of Crystal Growth **104** (1990) 108.

[9] M. Spiegel C. Zechner, B. Bitnar, G. Hahn, W. Jooss, P. Fath, G. Willeke, E. Bucher, H.-U. Höfs, C. Häßler, Solar Energy Materials and Solar Cells **55** (1998) 331.

[10] G. Hahn, W. Jooss, M. Spiegel, P. Fath, G. Willeke, E. Bucher, Proc. 26th IEEE PVSC, Anaheim (1997) 75.

[11] B.L. Sopori; X: Deng; J.P. Benner, A. Rohatgi, P. Sana, S.K. Estreicher, Y.K. Park, M.A. Roberson, Solar Energy Materials and Solar Cells **41/42** (1996) 159.

[12] G. Hahn, P. Geiger, P. Fath, E. Bucher, Proc. 28th IEEE PVSC, Anchorage (2000) 95.

[13] T. Pernau, M. Spiegel, G. Kragler, P. Fath, E. Bucher, Proc. 16th EC PVSEC, Glasgow (2000) 1373.